Journal of the Korean Physical Society, Vol. 59, No. 2, August 2011, pp. 1868∼1871

Systematic Investigation on Momentum Distributions of Projectile-like Fragments at E/A = 290 MeV

Sadao Momota*
Kochi University of Technology, Kochi 782-8502, Japan

Mitsutaka Kanazawa, Atsushi Kitagawa and Shinji Sato
National Institute of Radiological Sciences, Chiba 263-8555, Japan

(Received 26 April 2010)

A systematic investigation on the longitudinal and transverse momentum ($P_{\rm L}$ and $P_{\rm T}$) distributions of projectile-like fragments (PLFs) produced at intermediate energies has been performed experimentally. The momentum distributions of PLFs in a broad range of mass and charge, produced from 290 MeV/u Ar- and Kr-beams with various targets (C, Al, Nb, Tb and Au), were observed. The analysis of $P_{\rm L}$ distributions with an asymmetric Gaussian function provides the deceleration effect and the width of the distributions with good precision. A definite systematics is found in both the deceleration effect and the width. The broader width obtained at the low-momentum side indicates the contribution of multi-step processes at this energy. The target and energy dependencies of the induced momentum width are also shown. The analysis of $P_{\rm T}$ distributions with an off-centered Gaussian function provides not only the width, but also the orbital-deflection effect. In principle, the width is independent on the target, and is consistently reproduced based on the previously proposed formulation. In contrast, the deflection effect shows a strong target dependence. In the case of one-nucleon removed fragments, the main part of the deflection effect can be understood by the Coulomb repulsion. The systematics of the momentum distributions, shown in the present studies, is important for evaluating the production cross sections of PLFs. Especially, the $P_{\rm T}$ distribution is crucial to deduce production cross sections from the production rates of PLFs, which are observed at the forward angle within the limited angular acceptance.

PACS numbers: 29.25.-t, 25.40.-h
Keywords: Projectile fragmentation, Momentum distribution, Deceleration, Orbital-deflection
DOI: 10.3938/jkps.59.1868

I. INTRODUCTION

Radioactive nuclear beam (RNB) is one of the powerful tools to study nuclear physics, and has been applied to various other fields. The projectile fragmentation process is a powerful method to produce RNB with an energy higher than several tens of MeV/u. In order to prepare a well-defined RNB, it is required to accumulate knowledge on the production rates and their momentum distributions. Galactic cosmic rays include the component of heavy ions, whose energy distribution has a peak at around $E = 200 \sim 300$ MeV/u. It is estimated that the nuclear fragmentation process caused by the component would be one of the key processes to account for a risk to the health of astronauts during a long-term space mission [1].

The momentum distribution of projectile-like fragments (PLFs) reflects the reaction process in which PLFs are produced. At relativistic energies of $E >1$ GeV/u, the observed momentum distributions of PLFs are well reproduced by an isotropic Gaussian function. The width of the distribution can be understood based on the Fermi motion of removed nucleons [2]. A post acceleration effect has been found as a shift of the longitudinal momentum ($P_{\rm L}$) distribution for light PLFs at $E =$ 500 and 1000 MeV/u, and the effect has been used as a tool to investigate the nuclear mean fields [3]. At lower energies of $E \leq 100$ MeV/u, the observed momentum distribution was anisotropic. $P_{\rm L}$ distribution obtained at the low-momentum side is broader than that at the high-momentum side [4]. This broadening, found at the low-momentum side, implies the contribution of multi-step processes. In [4], the observed $P_{\rm L}$ distribution was analyzed with an asymmetric Gaussian function, and the systematic deceleration effect was also provided. Concerning the transverse momentum ($P_{\rm T}$), the observed width was broader than that of the $P_{\rm L}$ distribution, and an additional orbital dispersion effect was proposed to understand the anisotropy at $E \sim 100$ MeV/u in [5]. In order to confirm the reliability of a formulation introduced in [5], more systematic measurements of $P_{\rm T}$ distributions are required. Systematic information on the

*E-mail: momota.sadao@kochi-tech.ac.jp

momentum distribution of PLFs is required to provide the production cross sections of PLFs. Especially, information on the $P_{\rm T}$ distribution is crucial to deduce cross sections from the production rates of PLFs, which are observed at the forward angle within a limited angular acceptance.

Previous measurements were mainly performed at $E > 500$ MeV/u or $E < 100$ MeV/u, and for the $P_{\rm L}$ distribution. In the present study, the $P_{\rm T}$ distributions as well as the $P_{\rm L}$ distributions of PLFs, which were produced from 290 MeV/u Ar- and Kr-beams, were observed with various kinds of targets.

II. EXPERIMENTAL

^{40}Ar- and ^{84}Kr-beams accelerated up to 290 MeV/u were prepared by the HIMAC accelerator at NIRS. PLFs, produced from targets with various masses (C, Al, Nb, Tb, and Au), were observed. The thickness of the target was 1 mm for C, 0.8 mm for Al, 0.5 mm for Nb and Tb, and 0.333 mm for Au. The energy loss of the incident beams in the targets was at most 20 MeV/u, which is sufficiently small to observe the momentum distribution of PLFs. In order to identify the produced PLFs, the high-energy beam transport system SB2 [6] was applied as a doubly achromatic spectrometer. The momentum acceptance of the spectrometer was adjusted to be $\Delta P/\,{\rm P} = \pm 0.5\%$ and $\pm 0.25\%$, which was defined at the momentum dispersive focusing point F1, for Ar- and Kr-beam, respectively. By applying a 4D slit, which was located 3 m behind the target, the angular acceptance was defined to be ± 13 mrad in both $\theta_{\rm x}$ and $\theta_{\rm y}$.

In order to observe the $P_{\rm L}$ distributions, the magnetic rigidity of ISOL was varied stepwise over ranges of about $60 \sim 130\%$ ($70 \sim 110\%$) of that corresponding to the incident Ar (Kr) beam. The identification of PLFs was carried out by measuring time of flight (TOF) and energy deposit (dE) event by event. Two plastic scintillation counters, installed at F1 and the doubly achromatic focusing point F3, were used to measure TOF. A silicon counter, installed at F3, was used to measure dE. In order to obtain the production rate for each PLF, the measured fragment yield was normalized by the primary-beam intensity, and the thickness of the target, and was corrected by considering the finite momentum and angular acceptance of ISOL. The primary-beam intensity was monitored as the count of charged particles scattered from a thin foil, which was inserted at an upstream position of the target. The beam-intensity monitor was calibrated both before and after the main run. Except for the contribution of the statistics, the ambiguity in the calibration was mainly from that of the beam-intensity monitor, and its typical value was about $\pm 5\%$. Considering the charge-state distribution of PLFs in flight [7], the contributions of fragments, which were not fully stripped, were at most 0.6%, and negligible compared with other ambiguities.

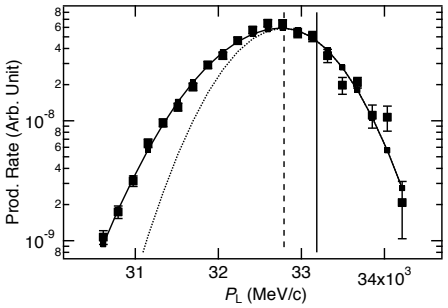

Fig. 1. Observed $P_{\rm L}$ distribution of ^{20}Ne produced from the reaction ^{40}Ar+C with fitting results. The solid and dashed lines correspond to the velocity of the primary beam and the center of $P_{\rm L}$ distribution, respectively.

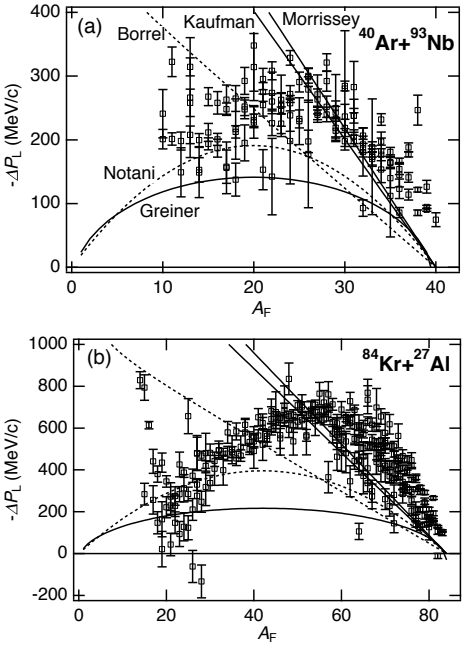

Fig. 2. Deceleration effect in the projectile fragmentation process. The systematics shown in the figures are described in [4].

III. EXPERIMENTAL RESULTS AND ANALYSIS

1. $P_{\rm L}$ distributions of PLFs

As shown in Fig. 1, the observed $P_{\rm L}$ distributions were successfully analyzed by an asymmetric Gaussian function, which was introduced in [4]. The function fitting provides the center of the $P_{\rm L}$ distribution and the width of the low- and high-momentum sides, $\sigma_{\rm Low}$ and $\sigma_{\rm High}$, respectively. In order to extract the deceleration effect in the fragmentation process ($-\Delta P_{\rm L}$), the contribution of the fragment-dependent energy loss in a target was subtracted from the observed results. The obtained deceleration effect is shown as a function of the mass of PLF ($A_{\rm F}$) with previously proposed systematics in Fig. 2. For heavier PLFs, the systematics proposed by Morrissey and Kaufman is plausible. However, no systematics reproduces the deceleration effect for lighter fragments.

Concerning the width, $\sigma_{\rm Low}$ is about $20 \sim 30\%$ larger

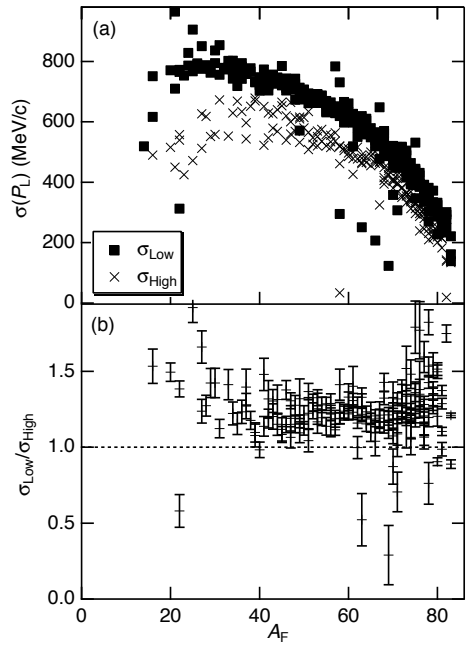

Fig. 3. Width of $P_{\rm L}$ distribution of PLF produced from Kr+C.

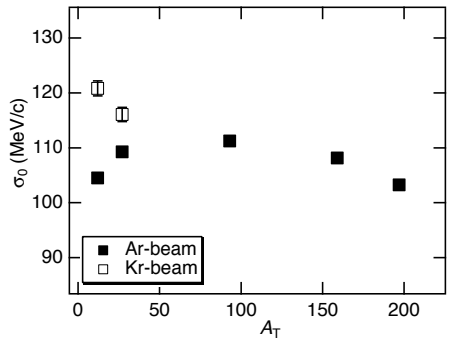

Fig. 4. Target dependence of σ_0.

than $\sigma_{\rm High}$, as shown in Fig. 3. It is implied from this result that the contribution of multi-step processes or highly excited states at $E = 290$ MeV/u cannot be negligible, but minor compared with that at 100 MeV/u [4]. The reduced momentum width (σ_0) obtained from $\sigma_{\rm High}$ based on [2] is independent on $A_{\rm F}$. σ_0 values averaged over all of the observed PLFs are shown for each reaction system in Fig. 4. This figure shows no obvious relations between σ_0 and the mass of fragment $A_{\rm T}$, while a larger σ_0 is obtained for Kr -beam compared with Ar-beam. The energy dependence of σ_0 is shown in Fig. 5. In the case of Ar beam, σ_0 is constant in the energy range of $E = 100 \sim 1000$ MeV/u. In contrast, σ_0 decreases with increasing energy of Kr beam. Also, the two recent results give relatively larger σ_0's compared with the previous results.

2. $P_{\rm T}$ distributions of PLFs

The observed $P_{\rm T}$ distributions of ^{39}Cl produced from Ar-beam are shown in Fig. 6. In the case of a light target (Al), the distribution has a peak at forward direction. Increasing $A_{\rm T}$, the distribution shifts sideway to develop an off-centered structure. It is indicated that heavier targets promote an orbital deflection of the projectile/fragment. The orbital-deflection effect is remarkable for few-particles removed fragments. It is plausible that this deflection effect would be from the Coulomb repulsion force against a target nucleus. For a numerical evaluation of the deflection effect, the observed $P_{\rm T}$ distribution is analyzed by an off-centered Gaussian function, defined as

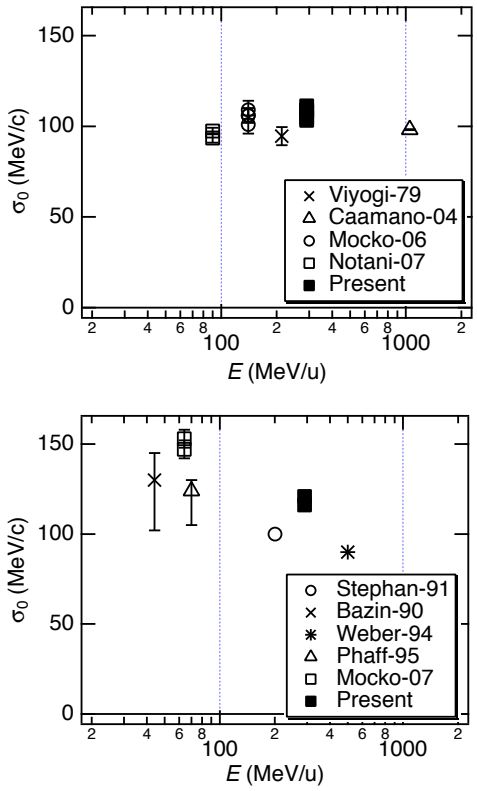

Fig. 5. (Color online) Energy dependence of σ_0.

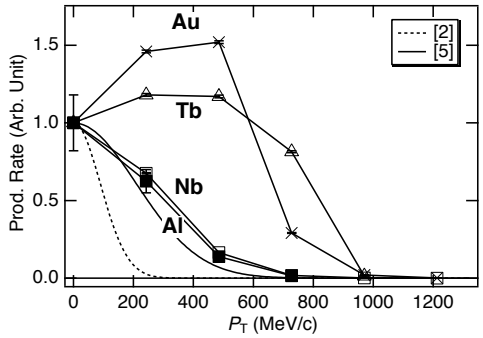

Fig. 6. $P_{\rm T}$ distribution of ^{39}Cl produced from Ar-beam.

$$Y(P_{\rm T}) = A\left\{\exp\left(-\frac{(P_{\rm T}-\Delta P_{\rm T})^2}{2\sigma_{\rm T}^2}\right)+\exp\left(-\frac{(P_{\rm T}+\Delta P_{\rm T})^2}{2\sigma_{\rm T}^2}\right)\right\}, \quad (1)$$

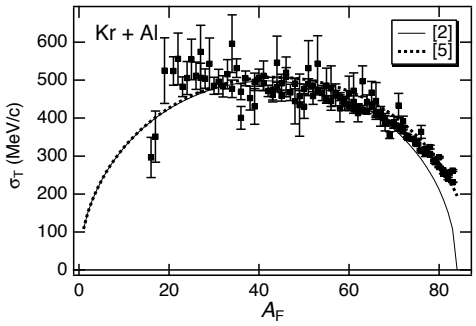

Fig. 7. $\sigma_{\rm T}$ of PLFs produced from Kr+Al.

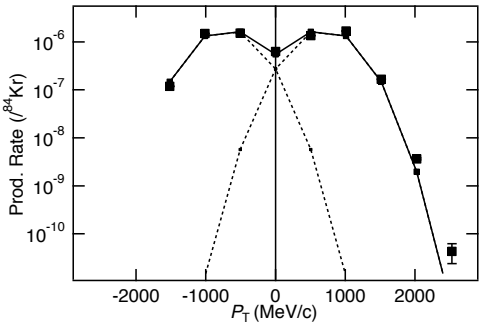

Fig. 8. $P_{\rm T}$ distribution of ^{83}Br produced from Kr+Au reaction analyzed with an off-centered Gaussian function.

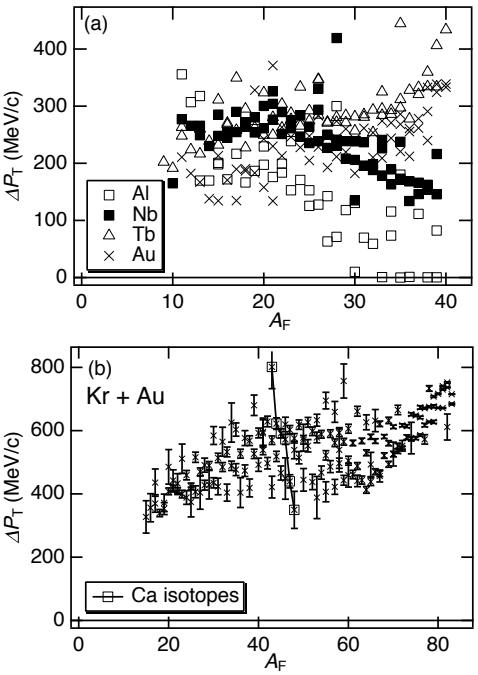

Fig. 9. Orbital-deflection effect of PLFs for (a) Ar-beam and (b) Kr-beam. As an example, a systematic fluctuatin $\Delta P_{\rm T}$ concerning isospin is shown for Ca isotopes in (b).

where $\Delta P_{\rm T}$ and $\sigma_{\rm T}$ denote the $P_{\rm T}$ of PLF induced by the orbital deflection and the width of the deflected $P_{\rm T}$ distribution, respectively. In order to consider the finite angular acceptance of ISOL, Eq. (1) is integrated over the angular acceptance mentioned in Sec. II.

In the case of a light target (Al), the observed $P_{\rm T}$ distributions is well reproduced without any orbital-deflection effect ($\Delta P_{\rm T} = 0$), also $\sigma_{\rm T}$, provided from function fitting, is consistent with that calculated based on Ref. 5, as shown in Fig. 7. In the case of heavier targets, the $P_{\rm T}$ distribution is successfully reproduced by Eq. (1) with $\sigma_{\rm T}$ provided from Ref. 5, as shown in Fig. 8.

In Fig. 9, the $\Delta P_{\rm T}$ is shown as a function of $A_{\rm F}$. In the case of Ar-beam (Fig. 9(a)), $\Delta P_{\rm T}$ shows an evident $A_{\rm F}$ dependence. No significant differences are found for PLFs with intermediate-mass $A_{\rm F} = 10 \sim 25$. In contrast, the orbital-deflection effect develops significantly for heavier PLFs ($A_{\rm F} > 25$). In the case of the Kr+Au reaction (Fig. 9(b)), the developed orbital-deflection effect is observed as well. The $\Delta P_{\rm T}$ of 1-p removed fragments ^{39}Cl and ^{83}Br, produced with an Au target, are 338.4 ± 0.4 and 715.5 ± 0.6 MeV/c, respectively. These values are comparable with $P_{\rm T}$ corresponding to the grazing angle originated by the Coulomb repulsion against the target nuclei. In addition, Fig. 9(b) shows a systematic fluctuation concerning the isospin. It is expected that the parameters, which characterize the fragmentation process such as the excitation energy and the impact parameter, would contribute to this behaviour.

IV. CONCLUSIONS

The $P_{\rm L}$ and $P_{\rm T}$ distributions of PLFs produced from Ar- and Kr-beams with 290 MeV/u were observed. Some features and systematics were extracted from an analysis of those distributions successfully. The asymmetric $P_{\rm L}$ distribution implies the contribution of multi-step processes at this energy. The reduced width was obtained from $\sigma_{\rm High}$, and its energy and target dependencies were indicated by comparing with previous results. An analysis of the $P_{\rm T}$ distribution by an off-centered Gaussian function extracted the orbital-deflection effect. It was evaluated that the Coulomb repulsion against the target nuclei plays a dominant role in the deflection effect. Further considerations are required to understand the systematic fluctuation concerning the isospin found in $\Delta P_{\rm T}$. The present results will also contribute to the experiment at the RIB facility and the development of the heavy-ion transport code.

ACKNOWLEDGMENTS

The present work was performed under the Research Project with Heavy Ions at NIRS-HIMAC (program # P-178).

REFERENCES

[1] Z. W. Lin, Phys. Rev. C **75**, 034609 (2007).
[2] A. S. Goldhaber, Phys. Lett. B **53**, 306 (1974).
[3] J. Benlliure *et al.*, Nucl. Phys. A **734**, 609 (2004).
[4] M. Notani *et al.*, Phys. Rev. C **76**, 044605 (2007).
[5] K. Van Bibber *et al.*, Phys. Rev. Lett. **43**, 840 (1979).
[6] S. Kouda *et al.*, in *Proceedings of 17th, Particle Accelerator Conf. (PAC)* (Vancouver, Canada 1997), p. 3822.
[7] C. Scheidenberger *et al.*, Nucl. Instrum. Methods Phys. Res. Sect. B **142**, 441 (1998).